RHEUMATOLOGY

Rheumatology 2017;56:2135–2144
doi:10.1093/rheumatology/kex329
Advance Access publication 5 September 2017

Original article

Patellofemoral morphology is not related to pain using three-dimensional quantitative analysis in an older population: data from the Osteoarthritis Initiative

Benjamin T. Drew[1,2,*], Michael A. Bowes[3,*], Anthony C. Redmond[1,2], Bright Dube[1,2], Sarah R. Kingsbury[1,2] and Philip G. Conaghan[1,2]

Abstract

Objectives. Current structural associations of patellofemoral pain (PFP) are based on 2D imaging methodology with inherent measurement uncertainty due to positioning and rotation. This study employed novel technology to create 3D measures of commonly described patellofemoral joint imaging features and compared these features in people with and without PFP in a large cohort.

Methods. We compared two groups from the Osteoarthritis Initiative: one with localized PFP and pain on stairs, and a control group with no knee pain; both groups had no radiographic OA. MRI bone surfaces were automatically segmented and aligned using active appearance models. We applied t-tests, logistic regression and linear discriminant analysis to compare 13 imaging features (including patella position, trochlear morphology, facet area and tilt) converted into 3D equivalents, and a measure of overall 3D shape.

Results. One hundred and fifteen knees with PFP (mean age 59.7, BMI 27.5 kg/m^2, female 58.2%) and 438 without PFP (mean age 63.6, BMI 26.9 kg/m^2, female 52.9%) were included. After correction for multiple testing, no statistically significant differences were found between groups for any of the 3D imaging features or their combinations. A statistically significant discrimination was noted for overall 3D shape between genders, confirming the validity of the 3D measures.

Conclusion. Challenging current perceptions, no differences in patellofemoral morphology were found between older people with and without PFP using 3D quantitative imaging analysis. Further work is needed to see if these findings are replicated in a younger PFP population.

Key words: magnetic resonance imaging, patellofemoral pain, active appearance modelling, 3D bone shape

CLINICAL SCIENCE

Rheumatology key messages

- No differences in joint morphology exist between older people with and without patellofemoral pain.
- Patellofemoral joint morphology differs significantly between men and women.

Introduction

Patellofemoral pain (PFP) refers to knee pain experienced in either the anterior or the retropatellar region [1]. Typically it presents during adolescence and early adulthood but can also be problematic for older adults [2]. The historical view that PFP is self-limiting has been challenged, with a number of studies demonstrating persistence of symptoms following diagnosis [3, 4]. This has led to the concept that PFP in some forms may represent a

[1]Leeds Institute of Rheumatic and Musculoskeletal Medicine, University of Leeds, [2]NIHR Leeds Biomedical Research Centre, Leeds and [3]Imorphics Ltd, Kilburn House, Manchester, UK

Submitted 20 March 2017; revised version accepted 31 July 2017

*Benjamin T. Drew and Michael A. Bowes contributed equally to this study

Correspondence to: Philip G. Conaghan, Leeds Institute of Rheumatic and Musculoskeletal Medicine, Chapel Allerton Hospital, Chapeltown Rd, Leeds LS7 4SA, UK.
E-mail: p.conaghan@leeds.ac.uk

pre-osteoarthritic state [5]. Currently, the aetiology of PFP remains unknown; however, the prevailing theory is that PFP is the result of structural malalignment and patellofemoral maltracking leading to excessive joint stress [6] and potential subchondral overload [7]. A number of studies have demonstrated structural differences within the patellofemoral joint (PFJ) between PFP and asymptomatic individuals [6, 8]. However, these findings were predominantly based on radiographic methods that have inherent limitations arising from their 2D methodology [9].

Recent literature has reported a number of MRI features associated with PFP [10]. Features such as patella medial–lateral position and patella tilt have been reported to be associated with PFP in small cohorts [10]. These studies typically used methods originally designed for radiographs and applied them to single MRI slices [9]. This type of '2D' measurement is not optimal, as it does not control for the position of the leg within the image. For example, a difference in patella alignment or shape may be genuine or may be caused by the object's pose, the combined relative position and rotation of the bones [11, 12]. From a practical perspective, these manual assessment methods are also user-dependent and time-consuming, making it difficult to analyse features for large datasets [13].

Using 3D quantitative analysis, utilizing active appearance models (AAMs) [14], provides a solution to these recognized imaging shortfalls. This analysis uses the statistics of shape and image information, calculated from a training set of images, and uses the resulting model to match to new images [15]. This automated segmentation is capable of accurate identification of the shape and appearance of bone, providing an accurate, faster and highly reliable solution for analysing large imaging datasets [14, 16]. A major benefit is that the 3D imaging measures are not influenced by the pose of the object [17].

Some previous studies have considered the shape of the PFJ using statistical shape models [18, 19], but these have included only asymptomatic individuals in small cohorts and have failed to consider the differences in the PFJ anatomy that exist between gender [20, 21]. The primary aim of this study was therefore to use modern image analysis technology to investigate the differences between 3D imaging features (based on existing radiographic measures) and overall bone shape for people with and without PFP in a large cohort, and to investigate whether any single 3D imaging feature, or combination of features, was associated with the presence of pain. As evidence suggests there are differences in PFJ morphology between genders [20–22], the secondary aim was to validate the measures used by exploring whether these features could significantly discriminate men and women.

Methods

Data were taken from the publically available Osteoarthritis Initiative (OAI) database, a multicentre, prospective, observational study with a database of 4796 people aged 45–79 years with both clinical and MRI data available. Details regarding the MRI protocol and sequences used are described elsewhere [23]. Cross-sectional clinical and MRI data were selected from the 24-month follow-up time point, being the first time point at which knee pain location was first assessed. The full OAI database can be found at: http://www.oai.ucsf.edu/datarelease/. All patients at each institutional review board-approved study site provided informed consent. The OAI study and the public use of all data used in the study were approved by the Committee on Human Research, University of California, San Francisco (Institutional Review Board approval number 10-00532). The study has been reported here in accordance to the Strengthening the Reporting of Observation Studies in Epidemiology guidelines [24].

Our PFP group was selected based on fulfilling all the following criteria: the presence of pain reported in the patella region by the participant (using a knee pain map); knee pain when using stairs—taken from the WOMAC pain subscale question; and a tibiofemoral joint Kellgren–Lawrence (KL) grade of 0 in at least one knee. Participants with any history of knee surgery in either knee, including replacement surgery, were excluded from the analysis. When bilateral knee pain was identified, the knee with the highest pain score with stair use was selected. If both knees had the same severity of pain, the right leg was chosen. One knee was selected for the control group based on fulfilling all the following: no pain in the patella region indicated by the participant; overall WOMAC score of 0; a numerical rating scale score of 0; KL grade of 0; and no history of surgery.

The bone surfaces for the trochlear femur and the subchondral patella were obtained by automatic segmenting using AAMs. The AAMs for the femur and patella joint surfaces (Fig. 1A) were built from an independent training set of 96 examples acquired using the double-echo steady-state with water excitation (DESS-we) MRI sequence chosen so as to contain examples from each stage of OA. Anatomical regions of subchondral bone were outlined on the mean patella and femur shapes using the correspondence points of the model, as previously described [16]. In this case, the PFJ surfaces were identified (Fig. 1A). An advantage of this method is that each automatic segmentation of an individual PFJ surface is automatically fitted with a dense set of anatomically corresponding landmarks, which can be used for measurements or for registration of examples.

This study relies on the ability of the AAM to accurately represent the 3D shape of the trochlear femur and the patella. Accuracy was assessed using 96 leave-one-out models, which were then fitted to the missing example. Distances from the known 3D surface to the AAM-searched surfaces were calculated as point-to-surface distance (millimetre) at each point in the model. Mean error (calculated using the root-mean-square method), and 95th percentile errors were calculated.

The patellar sub-region was defined as the subchondral area of the patella, together with a 'halo' of $\sim$10 mm around the subchondral plate. The femoral sub-region was defined as the trochlear subchondral region of the femur, using the anterior edge of the menisci as the

FIG. 1 Coordinate frame and model extent, facet regions

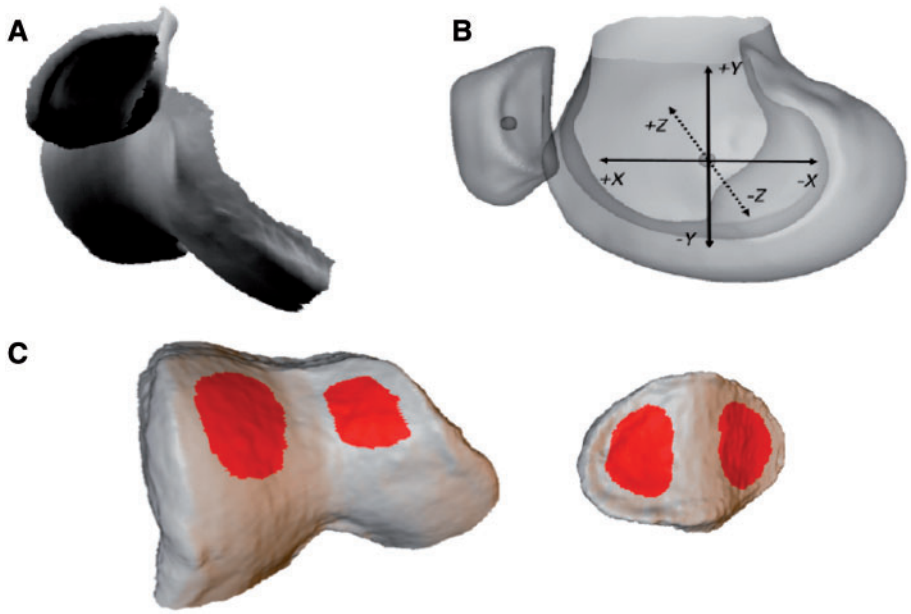

(**A**) Model extent—articulating surfaces plus small amount of bone surface beyond the articulating surface. Inferior boundary of trochlear femur is defined as the anterior edge of the menisci in the mean model. (**B**) Axes are taken from the mean model: X-axis: anterior–posterior (anterior positive); Y-axis: superior–inferior (superior negative); Z-axis: medial–lateral (lateral positive); coronal plane: looking along the X-axis (in the positive direction); axial plane: looking along the Y-axis (in the positive direction); sagittal plane: looking along the Z-axis (in the positive direction). (**C**) Facet regions of medial and lateral trochlear femur, and medial and lateral patella.

boundary of this region, plus a similar halo around the region. These two regions were combined into a single shape model, describing 95% of the variance in the shape, and the principal components for each individual PFJ surface were recorded.

We evaluated whether there were between-group differences in terms of the following 13 3D imaging features: patella medial–lateral position (millimetre), patella inferior–superior position (millimetre), patella anterior–posterior position (millimetre), medial patella facet area (square millimetre), lateral patella facet area (square millimetre), medial to lateral patella facet area (ratio), sulcus angle (°) [25], congruence angle (°) [25], medial trochlear inclination (°) [26], lateral trochlear inclination (°) [26], patella medial–lateral tilt (°), patella rotational alignment (°) and patellofemoral contact area (ratio). These 3D imaging features were converted from a range of standard MRI features derived from a systematic review of the literature [10] and shown to be the most commonly reported features.

An outline of the methods used to assess the imaging features, using the surfaces shown in Fig. 1A, are shown in Table 1. All PFJ surfaces were rigidly aligned with the mean shape, using a least squares fitting method, which fitted only the femur region. The X-, Y- and Z-axes were defined as anterior–posterior, superior–inferior and medial–lateral, respectively (Fig. 1B). The geometrical centre of gravity (COG) was calculated for patella and femur surfaces of each knee separately.

To determine the translation of the patella relative to the femur position, differences between the patella and femoral COGs were calculated along the X-, Y- and Z-axes. Angles between the medial and lateral facets of the patella and femur were calculated as follows: correspondence points within the facets were identified in the model as previously described (Fig. 1C) [16], and these masks were used to consistently identify these facets in each knee. For each knee bone surface, a plane was fitted to each of the medial patella, lateral patella, medial trochlea and lateral trochlea facets, and the angle calculated between the pairs of planes projected onto the X-, Y- and Z-axes.

Patella contact area was defined as the area of patella surface, which intersects with vectors normal to the trochlear femur at each correspondence point (based on the mean model; Fig. 1A), and expressed as a ratio of the total patella surface area. The sulcus angle, congruence angle and both the medial and lateral trochlear inclination angles were measured using planes established in the mean model (Table 1). The relationship between the area of the medial and lateral facets was expressed as a ratio (medial patella:lateral patella ratio). Patella tilt and rotational alignment were established by rigidly aligning each individual patella with the

Table 1 3D imaging features

PFJ Feature	Description	3D assessment method	Illustration
Patella medial–lateral position (mm)	Position of patella with respect to the femur in the medial–lateral direction (lateral = +ve)	Distance between the centre of gravity of the femur and patella in the coronal plane when projected onto the Z (medial–lateral) axis	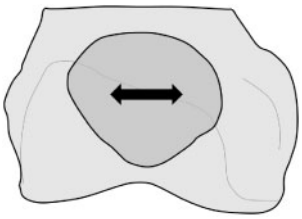
Patella inferior superior position (mm)	Position of patella with respect to the femur in the superior–inferior direction (superior = +ve)	Distance between the centre of gravity of the femur and patella when projected onto the Y (superior–inferior) axis	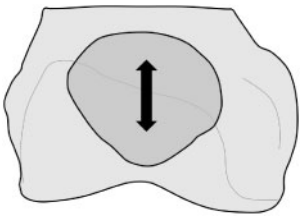
Patella anterior–posterior position (mm)	Position of patella with respect to the femur in the anterior–posterior direction (anterior = +ve)	Distance between the centre of gravity of the femur and patella when projected onto the X (anterior–posterior) axis	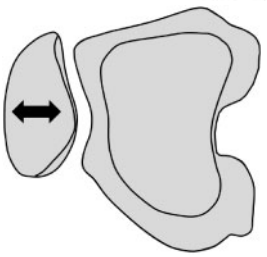
Medial patella facet area (mm^2)	3D surface area of medial facet	tAB area of the region shown as MP	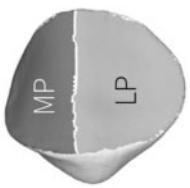
Lateral patella facet area (mm^2)	3D surface area of lateral facet	tAB area of the region shown as LP	See illustration for medial patella facet area
Medial patella facet to lateral patella facet ratio	The ratio of the medial and lateral facet area	The ratio of the medial and lateral facet area	See illustration for medial patella facet area
Sulcus angle (°)	The angle between the medial and lateral trochlear facets in the axial plane (viewed along the Y-axis)	The angle between planes fitted to the medial and lateral trochlear facets, viewed along the Y-axis (degrees)	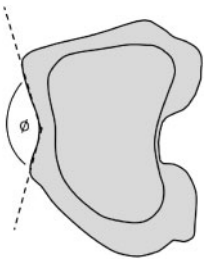
Congruence angle (°)	The difference in the sulcus angle and the angle between the patellar facets in the axial plane (viewed along the Y-axis)	Calculate the patellar facet angle as per the sulcus angle, but using the patellar facets. Congruence angle is sulcus angle minus the patellar facet angle	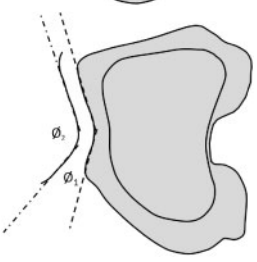

(continued)

TABLE 1 Continued

PFJ Feature	Description	3D assessment method	Illustration
Medial trochlear inclination (°)	The angle between the medial trochlear femur and the medial–lateral axis in the axial plane	The angle between a plane fitted to the medial trochlear of the femur (see Fig. 1) and the medial–lateral axis (X-axis), when viewed along the Y-axis	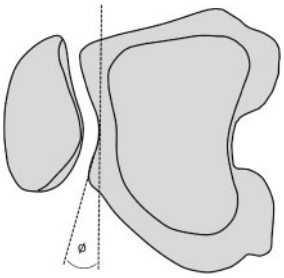
Lateral trochlear inclination (°)	The angle between the lateral trochlear femur and the medial–lateral axis in the axial plane	The angle between a plane fitted to the *lateral* trochlear of the femur (see Fig. 1) and the medial–lateral axis (X-axis), when viewed along the Y-axis	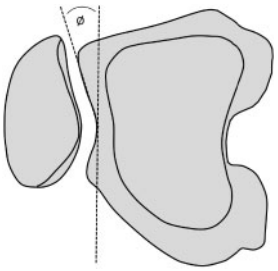
Patella medial–lateral tilt (°)	Rotation of the patella with respect to the femur in the axial plane	Following rigid alignment of the combined femur/patella surfaces using only the femur points, rotation of the patella around the Y-axis (+ve—rotated laterally, −ve rotated medially) compared with the mean position of the patella	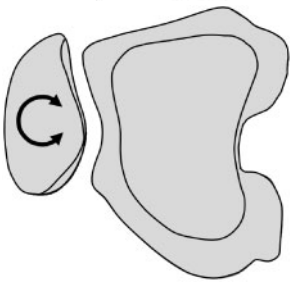
Patella rotational alignment (°)	Rotation of the patella with respect to the femur in the sagittal plane	Following rigid alignment of the combined femur/patella surfaces using only the femur points, rotation of the patella around the X-axis (+ve—rotated superiorly, −ve rotated inferiorly) compared with the mean position of the patella	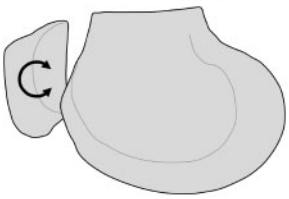
Patellofemoral contact area (ratio)	The percentage of patella coverage in relation to the femur	The percentage of patella surface which intersects with normal from the trochlear femur	

+ve: positive direction; −ve: negative direction; tAB: total area of subchondral bone; +ve: positive; PFJ: patellofemoral joint.

mean patella, and recording the rotation from the mean patella. For the direction of patella tilt and rotational alignment see Table 1.

Statistical analysis

Statistical analysis was carried out in SPSS version 21.0 (IBM Corp., Armonk, NY, USA). Descriptive statistics were used to describe the main characteristics of the study population and are presented as mean (S.D.) where appropriate for continuous variables, and frequency and percentages for categorical variables. For simple comparison between groups, independent-sample t-tests were used to compare the mean differences for all the 13 3D imaging features. Graphical exploration of the

data was performed to ensure that assumptions of normality were valid prior to performing the t-tests. To adjust for multiple comparisons, a Bonferroni correction was made and the level of significance set at $\alpha = 0.004$ (0.05/13).

Logistic regression models were used to identify whether any of the 3D imaging features, or a combination of features, were associated with PFP. Firstly, univariable models were performed on all 13 features to establish their individual association with PFP. For the two ratio variables (medial patella facet area to lateral patella facet and patellofemoral contact area) values were categorized based on the median value as lower than median and higher than median. This was then followed by multivariable models adjusted for gender. To achieve parsimony and also mitigate the effects of collinearity, the relationship of a selected number of 3D imaging features was considered for the multiple logistic models. The variable selection was based on the directed acyclic graph approach [27], which has been employed in other studies [13] to allow appropriate model specification. This approach results in parsimonious models being chosen without the risk of over-adjustment, although causality was not explicitly assumed from our models. An imaging feature was thus excluded from the model if one or more of the other imaging features were required for its formation and thus highly correlated. Accordingly, the medial patella facet to lateral patella facet ratio and patellofemoral contact area were omitted, as they are formed using both the medial and lateral patella facet area. The congruence angle and sulcus angle were omitted, as they are both built from the medial and lateral trochlear inclination. As some participants had a contralateral knee that was greater than KL zero, a sensitivity analysis was also performed, excluding all participants that did not have bilateral KL zero knees.

Linear discriminant analysis (LDA) of 3D shape explored whether any overall 3D shape or spatial position of the bones could discriminate between those with and without PFP, irrespective of the pre-selected 13 imaging features. The validity of this approach was examined by assessing if the method could discriminate between men and women, who are known to have different bone shapes [21]. Using the masks in Fig. 1, the bone surface of the trochlear femur and the subchondral patella were extracted from each knee (533 knees). These corresponding points were used to build a shape model of the isolated PF joint, which accounted for 98% of the shape variance. This resulted in 40 principal components. Subsequently, individual PF joints were represented as a series of principal components, which taken together provide an accurate representation of the 3D shape of the two bones and include the position and articulation of the femur and patella.

LDA of two groups expressed as 40 principal components is expected to find at least one hyperplane capable of separating out the groups (expressed as the distance between the two means of the groups projected onto the LDA hyperplane). To assess whether the separation achieved by LDA of the groups was better than that expected by chance we used a Monte Carlo experiment. For 10 000 repeats, each knee was randomly assigned a label in the same proportions as the dataset. A pseudo P-value is calculated from the number of repeats, which provides a better segmentation than the actual labelling.

Results

Based on our inclusion criteria we included 115 in the PFP group and 438 in the control group. The mean (S.D.) age was 59.7 (8.78) years for the PFP group and 63.6 (9.14) years for the control group, with 58.2% and 52.9% women in the PFP and control groups, respectively. The mean (S.D.) BMI was 27.5 (5.29) kg/m^2 for the PFP group and 26.9 (4.52) kg/m^2 for the control group.

Overall group comparison showed no statistically significant differences between people with and without PFP for any of the 13 3D imaging features (all $P > 0.004$) (Table 2). In addition, the sensitivity analysis similarly showed no statistically significant differences for any of the 3D imaging features (data not shown).

Univariable models showed no association between the individual 3D imaging features and PFP (Table 3). Results from the multivariable models revealed that combining 3D imaging features also showed no significant association with PFP ($P > 0.05$) and all the odds ratios remain close to the value of 1 indicating a lack of relationship to pain having adjusted for gender (Table 3).

The results of the LDA showed that the overall 3D shape was unable to significantly discriminate between the group with and without PFP showing a classification of 55.5%. The pseudo P-value from the Monte Carlo experiment was 0.79, indicating that the PFP/without PFP labelling separated out the groups no better than random chance. In contrast, the overall 3D shape was able to significantly discriminate between men and women with a classification of 90.6%. The pseudo P-values from the Monte Carlo experiment were <0.0001, indicating that it is unlikely that there is any labelling that separates the groups out better than gender.

The root-mean-square method mean point-surface accuracy of the femur and patella AAMs was 0.12 mm, 95th percentile 0.38 mm. The voxel sizes were 0.36 $\times$ 0.36 $\times$ 0.7 mm. This demonstrates that the model is accurate at almost all points to within 1 pixel on the screen.

Discussion

Our findings suggest that when commonly used patellofemoral imaging features are examined using careful 3D quantification, no statistically significant differences are found between a group with and without PFP. Furthermore, no single 3D imaging feature, or combination of features, was associated with the presence of PFP. The LDA experiment shows that, given bone shapes fitted with sub-voxel accuracy, there is nothing within the 3D shape of the joint able to classify the presence of PFP better than chance, at least using shape expressed as principal components.

TABLE 2 The mean differences between PFP and No PFP groups

Feature	Mean (S.D.)		Mean difference (95% CI)	P-value[a]
	PFP	No PFP		
Patellofemoral contact area (ratio)	0.41 (0.16)	0.41 (0.15)	0.00 (−0.03, 0.03)	0.83
Patella medial–lateral position (mm	−1.17 (2.25)	−1.02 (2.37)	− 0.15 (−0.63, 0.33)	0.54
Patella inferior–superior position (mm)	−21.03 (4.42)	−21.34 (4.66)	0.30 (−0.62, 1.23)	0.52
Patella anterior–posterior position (mm)	20.23 (2.04)	20.31 (1.93)	−0.08 (−0.48, 0.32)	0.69
Congruence angle (°)	9.04 (5.80)	8.68 (5.80)	0.36 (−0.84, 1.55)	0.56
Patella medial-lateral tilt (°)	−0.14 (3.33)	0.00 (3.31)	0.35 (−0.84, 1.55)	0.56
Medial trochlear inclination (°)	30.39 (4.27)	30.44 (4.02)	−0.05 (−0.89, 0.55)	0.90
Lateral trochlear inclination (°)	−25.52 (3.11)	−25.54 (2.70)	0.02 (−0.55, 0.59)	0.93
Patella rotational alignment (°)	−0.01 (2.53)	0.18 (2.77)	−0.18 (−0.75, 0.37)	0.63
Medial patella facet area (mm^2)	524.41 (81.57)	533.38 (85.12)	−8.96 (−26.34, 8.40)	0.31
Lateral patella facet area (mm^2)	667.45 (108.47)	681.48 (112.90)	−14.03 (−37.08, 9.02)	0.23
Medial patella facet to lateral facet (ratio)	0.79 (0.02)	0.79 (0.02)	0.00 (−0.00, 0.01)	0.18
Sulcus angle (°)	−124.09 (6.55)	−124.01 (5.80)	−0.07 (−1.30, 1.15)	0.91

[a]Independent samples *t* test. PFP: patellofemoral pain.

TABLE 3 The association between 13 3D imaging features and patellofemoral pain

Imaging feature	Univariable (unadjusted)		Multivariable (gender-adjusted)[a]	
	OR (95% CI)	P-value	OR (95% CI)	P-value
Patellofemoral contact area (lower)	0.97 (0.65, 1.47)	0.89	0.95 (0.63, 1.43)	0.79
Patella medial–lateral position (mm)	0.97 (0.89, 1.06)	0.54	0.97 (0.89, 1.06)	0.50
Patella inferior–superior position (mm)	1.02 (0.97, 1.06)	0.53	1.01 (0.97, 1.06)	0.65
Patella anterior–posterior position (mm)	0.98 (0.88, 1.09)	0.69	1.00 (0.89, 1.12)	0.99
Congruence angle (°)	1.01 (0.98, 1.05)	0.56	1.01 (0.98, 1.05)	0.52
Patella medial–lateral tilt (°)	0.98 (0.93, 1.05)	0.68	0.99 (0.93, 1.05)	0.64
Medial trochlear inclination (°)	0.99 (0.95,1.05)	0.90	0.99 (0.94, 1.04)	0.73
Lateral trochlear inclination (°)	1.00 (0.93, 1.08)	0.93	1.01 (0.94, 1.09)	0.80
Patella rotational alignment (°)	0.98 (0.90, 1.05)	0.51	0.97 (0.90, 1.05)	0.45
Medial patella facet area (mm^2)	0.99 (0.99, 1.00)	0.31	0.99 (0.99, 1.00)	0.65
Lateral patella facet area (mm^2)	0.99 (0.99, 1.00)	0.23	0.99 (0.99, 1.00)	0.49
Medial patella facet to lateral patella facet (lower)	0.55 (0.36, 0.83)	0.01	0.56 (0.36, 0.85)	0.01
Sulcus angle (°)	0.99 (0.96, 1.03)	0.91	0.99 (0.96, 1.03)	0.72
Gender (female)	1.24 (0.81, 1.88)	0.31		
Combined imaging features[b]				
Patella medial–lateral position (mm)			0.98 (0.89, 1.09)	0.73
Patella inferior–superior position (mm)			1.00 (0.95, 1.06)	0.93
Patella anterior–posterior position (mm)			1.03 (0.89, 1.18)	0.66
Patella medial-lateral tilt (°)			0.97 (0.89, 1.05)	0.47
Medial trochlear inclination (°)			0.99 (0.94, 1.07)	0.98
Lateral trochlear inclination (°)			1.03 (0.93, 1.14)	0.52
Patella rotational alignment (°)			0.96 (0.89, 1.05)	0.37
Medial patella facet area (mm^2)			1.01 (0.99, 1.03)	0.25
Lateral patella facet area (mm^2)			0.99 (0.98, 1.00)	0.18

[a]Adjusted for gender (female). [b]Variables removed: medial patella facet to lateral facet (ratio); sulcus angle (°); congruence angle (°); patellofemoral contact area (ratio). OR: odds ratio.

The finding that there is no association of the 3D imaging features with PFP is robust in this analysis but is in contrast to previous reports based on 2D imaging in the PFJ literature [6]. A recent review [28] of patellofemoral morphology in patellofemoral OA (PFOA) demonstrated strong evidence that PFOA is associated to trochlear (femoral) morphological features. A possible explanation for the contrast to our findings is highlighted by a previous study [29] of 30 knees assessed by MRI, which also found a lack of differences in femoral shape between people

Fig. 2 Apparent shape of the patella after small translations and rotations

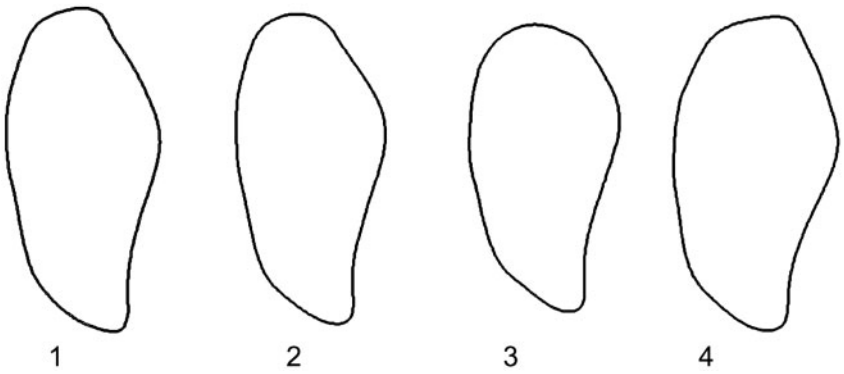

1) Shows the outline of the mean patella in the coronal plane; 2) outline at the same height in the coronal plane but with patella rotated by 10° around the medial-lateral axis; 3) outline at the same height but with the patella rotated by 10° around the anterior-posterior axis; 4) patella translated 10mm superiorly, plus both rotations (2) and (3). The overall outline of the patella varies despite being the same 3D shape and object.

with and without PFP. By subgrouping people with PFP into lateral and non-lateral maltracking groups, Harbaugh *et al*. [29] found that these subgroups lie on opposite sides of the healthy average, suggesting that underlying subgroups may be masking the differences between people with and without PFP [29]. A lack of established thresholds to define PFJ imaging feature subgroups did not allow this to be verified in the current study.

Further contrast to our findings is demonstrated by an MRI study of 240 knees [30] that showed that a medially inclined patella (similar to medial patella tilt in this analysis) was associated with less pain. This disparity may be because the assessments were performed on a single MR slice at the mid-point of the patella in the sagittal plane, and as noted previously, these methods may be open to measurement error by not controlling for relative limb position and orientation. Shibanuma *et al.* [12] showed that alterations in limb position led to statistically significant differences in the PFJ features recorded for both men and women. Patella alignment values including medial–lateral position and tilt have been shown to be influenced by the relative tibial and femoral rotation and varus angulation [11], while single slices along one plane are known to misrepresent the true anatomy of the PFJ [31] (see Fig. 2).

All the PFJ imaging features employed in the current study have been published previously [26, 30, 32, 33]. Our findings are comparable to a previous study that analysed trochlear morphology in 881 middle-aged knees using MRI [34]. Stefanik *et al.* [34] reported similar values for sulcus, lateral trochlear inclination and medial inclination angles of 130.9°, 25° and 24.4°, respectively, though the novel assessment methods used here preclude direct comparison with that study. This is because, in contrast to traditional methods, the geometrical COG was used here as a more representative reference point for 3D shape. The use of statistical shape models has also been applied previously in the PFJ [18]; however, this is the first time these methods have been employed on a large, symptomatic group with a comprehensive range of traditional features converted into their 3D equivalents.

A growing evidence base suggests that PFJ imaging features are influenced by gender [20–22]. Validation of these new 3D imaging features was achieved by using the shape data from the 3D imaging features, coded as principal components, showing that gender is classified at a 90% level of accuracy. This is similar to the classification of 93.5% in sex determination using 3D CT features of the patella *in vitro* [21]. Our model expands on this work by applying 3D MR imaging features from both the patella and femoral trochlea *in vivo*. Given that there are significant differences by gender for PFJ imaging features, it seems likely that previous studies have been affected by a mix of genders within their sample. A recent review [10] of the imaging literature in PFP shows that of studies including mixed gender cohorts, 80% failed to report women and men separately. Therefore previous studies may simply have been describing differences related to their gender mix. As a result, it is recommended that future studies follow the lead of recent studies [35] by reporting gender separately or conducting single gender analyses.

There are limitations to this study. This analysis was conducted on a sample older than a typical PFP patient and thus caution is advised in extrapolating these findings to a younger population. While all selected patients had KL grade 0 within the tibiofemoral joint, there were no lateral or skyline X-rays available to view the PFJ radiographically. Without lateral or skyline X-rays we cannot assert that all participants were without radiographic PFOA; however, previous studies have suggested that in the absence of OA in the tibiofemoral joint, ~75% of this age cohort will have no other compartmental OA [36, 37]. Also, the features were based on MRI images taken in

non-weight bearing with no knee flexion. Weight bearing and knee flexion are known to influence the features observed [7, 10]. In the current study, participants were selected based on clinically determined PFP associated with localized pain to the patella and pain on descending stairs, features known to have a strong clinical association with the diagnosis of PFP [38]. PFP was based on a single time point (24 months) and pain based on a dichotomized value (pain/no pain) rather than a graded severity scale. Despite being a large sample size compared with previous literature, the sample size is probably still small considering the high dimensionality of the data, which may have limited the power of the analyses to detect differences.

Our analysis included a range of quantitative 3D measures, together with an examination of the principal components from the associated shape model. The use of principal component analysis for one of the measures may have resulted in the loss of some 3D information, and it is possible that other advanced methods of shape analysis and machine learning could reveal a relationship that our methods cannot.

In conclusion, using 3D quantitative analysis, no statistically significant differences were found between people with and without PFP. These 3D findings are in contrast to the current perception, which has relied on studies using what are effectively 2D measurements applied with a lack of consistent joint positioning. Analyses of the overall 3D shape in relation to gender validates these novel measures and suggests future PFP cohort analyses should be stratified for gender. Further work is needed to assess whether 3D quantitative analysis can discriminate shape differences related to PFP in a younger population, more characteristic of PFP.

Acknowledgements

The OAI is a public-private partnership comprising five contracts (N01-AR-2-2258; N01-AR-2-2259; N01-AR-2-2260; N01-AR- 2-2261; N01-AR-2-2262) funded by the National Institutes of Health, a branch of the Department of Health and Human Services, and conducted by the OAI Study Investigators. Private funding partners include Merck Research Laboratories, Novartis Pharmaceuticals Corporation, GlaxoSmithKline and Pfizer, Inc. Private sector funding for the OAI is managed by the Foundation for the National Institutes of Health. This manuscript was prepared using an OAI public use data set and does not necessarily reflect the opinions or views of the OAI investigators, the National Institutes of Health, or the private funding partners.

P.G.C., S.K. and A.R. are in part supported through the National Institute for Health Research (NIHR) Leeds Biomedical Research Centre and A.R. is an NIHR Senior Investigator. This paper presents independent research funded by the NIHR. The views expressed are those of the authors and not necessarily those of the NHS, the NIHR or the Department of Health. We would also like to thank Dr Andrew Barr for his advice and comments on the manuscript and Dr Elizabeth Hensor for her statistical support.

Funding: This work was supported by funding from a National Institute for Health Research (NIHR) Clinical Doctoral Research Fellowship (CDRF-2013-04-044); the Arthritis Research UK Experimental Osteoarthritis Treatment Centre (Ref. 20083); and the Arthritis Research UK Centre for Sport, Exercise and Osteoarthritis (Ref. 20194).

Disclosure statement: Michael Bowes is an employee and shareholder of Imorphics Ltd, a wholly owned subsidiary of Stryker Corp. All other authors have nothing to disclose.

References

1 Callaghan MJ, Selfe J. Patellar taping for patellofemoral pain syndrome in adults. Cochrane Database Syst Rev 2012;4:CD006717.

2 Crossley KM, Callaghan MJ, van Linschoten R. Patellofemoral pain. Br J Sports Med 2016;50:247–50.

3 Nimon G, Murray D, Sandow M, Goodfellow J. Natural history of anterior knee pain: a 14- to 20-year follow-up of nonoperative management. J Pediatr Orthop 1998;18:118–22.

4 Stathopulu E, Baildam E. Anterior knee pain: a long-term follow-up. Rheumatology 2003;42:380–2.

5 Crossley KM. Is patellofemoral osteoarthritis a common sequela of patellofemoral pain? Br J Sports Med 2014;48:409–10.

6 Powers CM, Bolgla LA, Callaghan MJ, Collins N, Sheehan FT. Patellofemoral pain: proximal, distal, and local factors—Second International Research Retreat, August 31–September 2, 2011, Ghent, Belgium. J Orthop Sports Phys Ther 2012;42:A1–54.

7 Besier TF, Draper C, Pal S *et al*. Imaging and musculoskeletal modeling to investigate the mechanical etiology of patellofemoral pain. In: Sanchis-Alfonso V, ed. Anterior Knee Pain and Patellar Instability. London: Springer, 2011: 269–86.

8 Witvrouw E, Callaghan MJ, Stefanik JJ *et al*. Patellofemoral pain: consensus statement from the 3rd International Patellofemoral Pain Research Retreat held in Vancouver, September 2013. Br J Sports Med 2014;48:411–4.

9 Wilson T. The measurement of patellar alignment in patellofemoral pain syndrome: are we confusing assumptions with evidence?. J Orthop Sports Phys Ther 2007;37:330–41.

10 Drew BT, Redmond AC, Smith TO, Penny F, and Conaghan PG. Which patellofemoral joint imaging features are associated with patellofemoral pain? Systematic review and meta-analysis. Osteoarthritis Cartilage 2015;24:224–36.

11 Katchburian MV, Bull AM, Shih YF, Heatley FW, Amis AA. Measurement of patellar tracking: assessment and analysis of the literature. Clin Orthop Relat Res 2003;412:241–59.

12 Shibanuma N, Sheehan FT, Stanhope SJ. Limb positioning is critical for defining patellofemoral alignment and femoral shape. Clin Orthop Relat Res 2005;(434):198–206.

13 Barr AJ, Dube B, Hensor EM *et al*. The relationship between clinical characteristics, radiographic osteoarthritis and 3D bone area: data from the Osteoarthritis Initiative. Osteoarthritis Cartilage 2014;22:1703–9.

14 Cootes TF, Edwards GJ, Taylor CJ. Active apperance models. IEEE Trans Pattern Anal Mach Intell 2001;23:681–5.

15 Vincent G, Wolstenholme C, Scott I, Bowes M. Fully automatic segmentation of the knee joint using active appearance models. In: van Ginneken B, Murphy K, Heimann T, Pekar V, Deng X, (eds). Medical Image Analysis for the Clinic: A Grand Challenge. USA: CreateSpace, 2010; 224–30.

16 Bowes MA, Vincent GR, Wolstenholme CB, Conaghan PG. A novel method for bone area measurement provides new insights into osteoarthritis and its progression. Ann Rheum Dis 2015;74:519–25.

17 Williams TG, Vincent G, Bowes MA *et al*. Automatic segmentation of bones and inter-image anatomical correspondence by volumetric statistical modelling of knee MRI. In 7th IEEE International Symposium on Biomedical Imaging: From Nano to Macro. Institute of Electrical and Electronics Engineers, 2010, 432–35.

18 Fitzpatrick CK, Baldwin MA, Laz PJ *et al*. Development of a statistical shape model of the patellofemoral joint for investigating relationships between shape and function. J Biomech 2011;44:2446–52.

19 Fitzpatrick CK, Baldwin MA, Rullkoetter PJ, Laz PJ. Combined probabilistic and principal component analysis approach for multivariate sensitivity evaluation and application to implanted patellofemoral mechanics. J Biomech 2011;44:13–21.

20 Faber SC, Eckstein F, Lukasz S *et al*. Gender differences in knee joint cartilage thickness, volume and articular surface areas: assessment with quantitative three-dimensional MR imaging. Skeletal Radiol 2001;30:144–50.

21 Mahfouz M, Badawi A, Merkl B *et al*. Patella sex determination by 3D statistical shape models and nonlinear classifiers. Forensic Sci Int 2007;173:161–70.

22 Csintalan RP, Schulz MM, Woo J, McMahon PJ, Lee TQ. Gender differences in patellofemoral joint biomechanics. Clin Orthop Relat Res 2002;402:260–9.

23 Peterfy CG, Schneider E, Nevitt M. The osteoarthritis initiative: report on the design rationale for the magnetic resonance imaging protocol for the knee. Osteoarthritis Cartilage 2008;16:1433–41.

24 Von Elm E, Altman DG, Egger M *et al*. The Strengthening the Reporting of Observational Studies in Epidemiology (STROBE) statement: guidelines for reporting observational studies. Prev Med 2007;45:247–51.

25 Thomee R, Renström P, Karlsson J, Grimby G. Patellofemoral pain syndrome in young women. Scand J Med Sci Sports 1995;5:245–51.

26 Teng HL, Chen YJ, Powers CM. Predictors of patellar alignment during weight bearing: an examination of patellar height and trochlear geometry. Knee 2014;21:142–6.

27 Shrier I, Platt RW. Reducing bias through directed acyclic graphs. BMC Med Res Methodol 2008;8:70.

28 Macri EM, Stefanik JJ, Khan KM, Crossley KM. Is tibiofemoral or patellofemoral alignment or trochlear morphology associated with patellofemoral osteoarthritis? A systematic review. Arthritis Care Res 2016;68:1453–70.

29 Harbaugh CM, Wilson NA, Sheehan FT. Correlating femoral shape with patellar kinematics in patients with patellofemoral pain. J Orthop Res 2010;28:865–72.

30 Tanamas SK, Teichtahl AJ, Wluka AE *et al*. The associations between indices of patellofemoral geometry and knee pain and patella cartilage volume: a cross-sectional study. BMC Musculoskelet Disord 2010;11:87.

31 Staubli HU, Durrenmatt U, Porcellini B, Rauschning W. Anatomy and surface geometry of the patellofemoral joint in the axial plane. J Bone Joint Surg Br 1999;81:452–8.

32 Farrokhi S, Colletti PM, Powers CM. Differences in patellar cartilage thickness, transverse relaxation time, and deformational behavior: a comparison of young women with and without patellofemoral pain. Am J Sports Med 2011;39:384–91.

33 Powers CM, Ward SR, Fredericson M, Guillet M, Shellock FG. Patellofemoral kinematics during weight-bearing and non-weight-bearing knee extension in persons with lateral subluxation of the patella: a preliminary study. J Orthop Sports Phys Ther 2003;33:677–85.

34 Stefanik JJ, Roemer FW, Zumwalt AC *et al*. Association between measures of trochlear morphology and structural features of patellofemoral joint osteoarthritis on MRI: the MOST study. J Orthop Res 2012;30:1–8.

35 Pattyn E, Mahieu N, Selfe J *et al*. What predicts functional outcome after treatment for patellofemoral pain? Med Sci Sports Exerc 2012;44:1827–33.

36 Hinman RS, Lentzos J, Vicenzino B, Crossley KM. Is patellofemoral osteoarthritis common in middle-aged people with chronic patellofemoral pain? Arthritis Care Res 2014;66:1252–7.

37 Peat G, Duncan RC, Wood LR, Thomas E, Muller S. Clinical features of symptomatic patellofemoral joint osteoarthritis. Arthritis Res Ther 2012;14:R63.

38 Cook C, Mabry L, Reiman MP, Hegedus EJ. Best tests/clinical findings for screening and diagnosis of patellofemoral pain syndrome: a systematic review. Physiotherapy 2012;98:93–100.